JOURNAL OF VIROLOGY, Apr. 2007, p. 3922–3932 Vol. 81, No. 8
0022-538X/07/$08.00+0 doi:10.1128/JVI.02091-06

Human Coronavirus 229E Papain-Like Proteases Have Overlapping Specificities but Distinct Functions in Viral Replication▽

John Ziebuhr,[1] Barbara Schelle,[2] Nadja Karl,[1,2] Ekaterina Minskaia,[1] Sonja Bayer,[2] Stuart G. Siddell,[3] Alexander E. Gorbalenya,[4] and Volker Thiel[5]*

Centre for Cancer Research and Cell Biology, School of Biomedical Sciences, The Queen's University of Belfast, Belfast, United Kingdom[1]; Institute of Virology and Immunology, University of Würzburg, Würzburg, Germany[2]; Department of Cellular and Molecular Medicine, School of Medical and Veterinary Sciences, University of Bristol, Bristol, United Kingdom[3]; Department of Medical Microbiology, Leiden University Medical Center, Leiden, The Netherlands[4]; and Research Department, Kantonal Hospital St. Gallen, St. Gallen, Switzerland[5]

Received 25 September 2006/Accepted 16 January 2007

Expression of the exceptionally large RNA genomes of CoVs involves multiple regulatory mechanisms, including extensive proteolytic processing of the large replicase polyproteins, pp1a and pp1ab, by two types of cysteine proteases: the chymotrypsin-like main protease and papain-like accessory proteases (PL^{pro}s). Here, we characterized the proteolytic processing of the human coronavirus 229E (HCoV-229E) amino-proximal pp1a/pp1ab region by two paralogous PL^{pro} activities. Reverse-genetics data revealed that replacement of the $PL2^{pro}$ active-site cysteine was lethal. By contrast, the $PL1^{pro}$ activity proved to be dispensable for HCoV-229E virus replication, although reversion of the $PL1^{pro}$ active-site substitution to the wild-type sequence after several passages in cell culture indicated that there was selection pressure to restore the $PL1^{pro}$ activity. Further experiments showed that both $PL1^{pro}$ and $PL2^{pro}$ were able to cleave the nsp1-nsp2 cleavage site, with $PL2^{pro}$ cleaving the site less efficiently. The $PL1^{pro}$-negative mutant genotype could be stably maintained in cell culture when the nsp1-nsp2 site was replaced by a short autoproteolytic sequence, suggesting that the major driving force for the observed reversion of the $PL1^{pro}$ mutation was the requirement for efficient nsp1-nsp2 cleavage. The data suggest that the two HCoV-229E PL^{pro} paralogs have overlapping substrate specificities but different functions in viral replication. Within the tightly controlled interplay of the two protease activities, $PL2^{pro}$ plays a universal and essential proteolytic role that appears to be assisted by the $PL1^{pro}$ paralog at specific sites. Functional and evolutionary implications of the differential amino-terminal polyprotein-processing pathways among the main CoV lineages are discussed.

Expression of positive-strand RNA virus genomes generally starts with the translation of the incoming viral RNA to produce large precursor proteins that are co- and posttranslationally processed by viral and, in some cases, cellular proteases. The proteolytic release of intermediate and mature processing products, which may have diverse functions in different phases of viral replication, is spatially and temporally coordinated. Protease activities can therefore be viewed as key regulators of the life cycles of positive-strand RNA viruses.

The positive-strand RNA coronaviruses (CoVs) have evolved a most complex pattern of polyprotein processing and regulation (64, 66). The 5′-terminal two-thirds of the giant 30-kb genome is occupied by two overlapping open reading frames (ORFs), called 1a and 1b, which together form the viral replicase gene and whose translation results in the production of two large polyproteins. ORF1a encodes polyprotein 1a (pp1a), and ORFs 1a and 1b encode pp1ab. The biosynthesis of pp1ab involves a ribosomal frameshift at the ORF1a-ORF1b junction during translation (9, 10). As many as 15 or 16 processing end products, which are called nonstructural proteins (nsps), are proteolytically released from pp1a/pp1ab (64, 66). Together with a number of cellular proteins (51) and the viral nucleocapsid (N) protein (1, 49), the nsps are believed to form a membrane-bound multienzyme complex, which is called the replicase-transcriptase complex (47, 52).

The proteins located downstream (i.e., carboxy terminal) of nsp5 in pp1a/pp1ab include key replicative enzymes of the virus, such as RNA-dependent RNA polymerase (nsp12) (12), RNA helicase (nsp13) (50), exoribonuclease (nsp14) (42), endoribonuclease (nsp15) (6, 31), and putative methyltransferase (nsp16) activities (53, 64). They also include several small proteins, nsp7 to nsp10, which typically have RNA-binding activities (18, 32, 40, 56, 63) and therefore are believed to be involved in viral RNA synthesis, as well as the hydrophobic, probably membrane-spanning protein nsp6. Because of its key role in the proteolytic release of all these proteins, the nsp5-associated cysteine protease activity is critically involved in viral replication and therefore is often referred to as the CoV "main protease" (M^{pro}) (64, 66). The nsp5-associated M^{pro} has a chymotrypsin-like fold that is fused to a unique carboxy-terminal domain and displays a narrow substrate specificity that resembles that of picornavirus 3C proteases (2, 3, 21, 66). The M^{pro}-mediated processing pathways are well conserved: in all CoVs, M^{pro} cleaves as many as 11 pp1a/pp1ab sites to produce a total of 13 mature proteins. Consequently, the patterns of M^{pro}-mediated processing are likely to be very similar for all CoVs (64).

Proteins upstream of nsp5 include (i) the hydrophobic, membrane-bound nsp4; (ii) two large multidomain proteins (nsp2 and nsp3); and (iii) the amino-terminal product, nsp1,

* Corresponding author. Mailing address: Kantonal Hospital St. Gallen, Research Department, 9007 St. Gallen, Switzerland. Phone: 41-71-4942843. Fax: 41-71-4946321. E-mail: volker.thiel@kssg.ch.

▽ Published ahead of print on 24 January 2007.

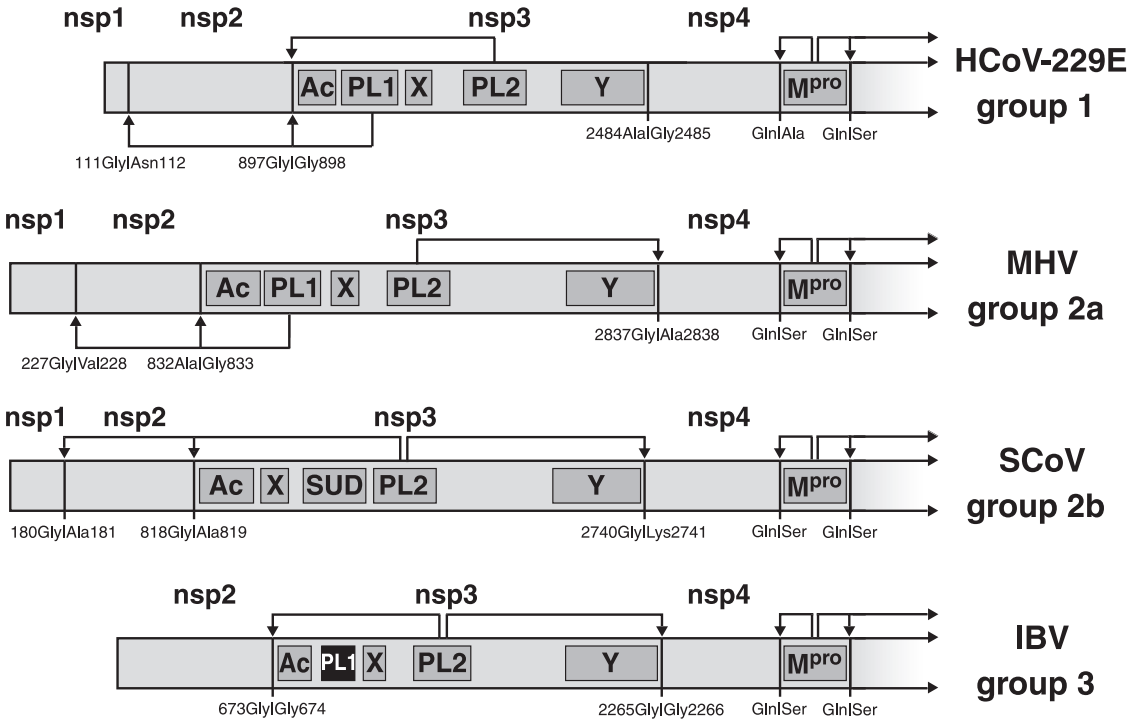

FIG. 1. CoV PL^{pro}-mediated polyprotein processing. The pp1a/pp1ab amino-terminal regions of HCoV-229E (group 1), MHV (group 2a), SARS-CoV (SCoV, group 2b), and IBV (group 3) are shown with the previously identified processing end products nsp1 to nsp4 and the corresponding cleavage sites (P1 and P′ residues are indicated). The sites processed by specific protease domains are indicated by arrows. P1 and P′ residues are given. Ac, acidic domain; PL1, papain-like protease 1; X, ADP-ribose-1″phosphatase; PL2, papain-like protease 2; Y, domain with conserved Cys/His residues and putative transmembrane regions; SUD, SARS-CoV specific domain.

which is found in most, but not all, CoVs (Fig. 1). The amino-proximal pp1a/pp1ab proteins nsp1 to nsp3 are relatively poorly conserved (53, 67), and there is evidence that some of these proteins, or their subdomains, are not essential (11, 25, 43). Hence, the nsp3-associated cysteine proteases PL1^{pro} and PL2^{pro}, which control the proteolytic processing of this pp1a/pp1ab region, are also referred to as CoV "accessory proteases" (64, 66). nsp4 is sandwiched between the autoproteolytically released proteins nsp3 and nsp5, and accordingly, its release from pp1a/pp1ab is under the control of both main and accessory proteases.

The multidomain protein nsp3 is the largest CoV replicative protein (67). It has a size of ~1,700 to 1,900 amino acids and includes one or two proteases, called PL1^{pro} and PL2^{pro}, that adopt a papain-like fold, with amino- and carboxy-terminal domains connected by a Zn ribbon structure (22, 29, 44). PL1^{pro} and PL2^{pro} reside upstream and downstream, respectively, of the conserved ADP-ribose-1″-phosphatase (ADRP) domain (19, 22, 43, 46, 53) whose biological function is not yet known (Fig. 1). Several other domains were provisionally identified in nsp3, with two of them, an acidic (Ac) domain at the amino terminus and a Cys/His-rich domain at the carboxy terminus (the Y domain), being conserved in all CoVs (67). Also, PL2^{pro} is conserved in all CoVs. The protease is amino-terminally extended by a small ubiquitin-like (Ubi) domain that probably modulates the PL2^{pro} deubiquitinating activity (5, 44, 54). In contrast, PL1^{pro} was identified only in CoVs belonging to genetic group 1 and subgroup 2a. Subgroup 2b CoVs, including severe acute respiratory syndrome (SARS)-CoV, do not encode a PL1^{pro} (39, 45, 53, 60), whereas group 3 CoVs (prototype, infectious bronchitis virus [IBV]) possess a PL1^{pro} remnant that lacks proteolytic activity (67).

Besides differences in the domain organization of nsp1 to nsp3, there are also differences in the proteolytic-processing pathways among the various groups and subgroups of CoVs. Thus, for example, in the CoV groups 2b and 3, which specify a single papain-like protease activity, the PL2^{pro} activity is responsible for the processing of the entire amino-proximal region to produce two or three mature proteins (27, 36, 37, 60). These PL2^{pro} cleavage sites have three strictly conserved residues at their P4 to P1 positions (60). By contrast, in CoVs encoding two PL^{pro}s, the regulation of the proteolytic-processing pathways seems to be more complex. For example, in mouse hepatitis virus (MHV), the prototype of CoV group 2a, PL1^{pro} cleaves the nsp1-nsp2 and nsp2-nsp3 sites, while PL2^{pro} cleaves the nsp3-nsp4 site (4, 7, 8, 15, 24, 34, 57). Accordingly, the MHV PL1^{pro} and PL2^{pro} cleavage sites resemble each other only remotely in that both of them have small amino acid residues at their P2 and/or P1 positions. In human CoV 229E (HCoV-229E), a group 1 CoV, the situation is again different. Here, the nsp1-nsp2 site was reported to be processed by PL1^{pro}, whereas the nsp2-nsp3 site can be processed by either PL1^{pro} or PL2^{pro}, with PL2^{pro} being the dominant activity (28, 67). Accordingly, these sites, and the yet-to-be-verified HCoV-229E nsp3-nsp4 site, are more similar to each other, resembling the situation found in CoVs encoding just one active PL^{pro} (60).

In this study, we have characterized the proteolytic regula-

tion of HCoV-229E nsp1 synthesis using reverse genetics. The HCoV-229E nsp1 belongs to an uncharacterized protein family that is conserved in group 1 CoVs. It is distinct from the nsp1 protein family of group 2 CoVs, which was recently shown for MHV to affect diverse host cell functions (33). In our study, we sought to answer the question of whether, and to what extent, the two PL^{pro} activities were involved in the proteolytic release of nsp1. We used the HCoV-229E reverse-genetics system (58) to produce mutants in which one of the protease activities, either $PL1^{pro}$ or $PL2^{pro}$, was abolished by codon mutagenesis of the active-site nucleophile. The data show that inactivation of $PL2^{pro}$ is lethal, whereas the $PL1^{pro}$ activity is dispensable for HCoV-229E replication, as demonstrated by Northern blot analysis of viral RNA synthesis and the rescue of a viable $PL1^{pro}$-negative mutant. However, upon passage in cell culture, the $PL1^{pro}$-negative mutant reverted to the wild-type sequence, indicating selective pressure to restore the $PL1^{pro}$ activity. Our further analysis revealed that $PL2^{pro}$ is able to cleave the nsp1-nsp2 site, although less efficiently than does $PL1^{pro}$. Finally, by uncoupling cleavage of the nsp1-nsp2 site from the two PL^{pro} activities, we managed to stably maintain the $PL1^{pro}$-negative mutant genotype in cell culture. This suggests that the major driving force for the reversion of the $PL1^{pro}$ mutation was the requirement for an efficient cleavage of the nsp1-nsp2 site. Taken together, our data provide further evidence for overlapping substrate specificities of the $PL1^{pro}$ and $PL2^{pro}$ domains in HCoV-229E. In this functional cooperation, the essential $PL2^{pro}$ domain plays a major and clearly dominant proteolytic role, whereas the dispensable paralogous $PL1^{pro}$ may have evolved to at least partially liberate the $PL2^{pro}$ domain from its role in efficient nsp1-nsp2 processing.

MATERIALS AND METHODS

Viruses and cells. MRC-5 and CV-1 cells were purchased from the European Collection of Cell Cultures. D980R cells were a kind gift from G. L. Smith, Imperial College, London, United Kingdom. BHK-HCoV-N cells, expressing the HCoV-229E nucleocapsid protein under the control of the TET/ON system (Clontech), have been described previously (49, 62). All cells were maintained in minimal essential medium supplemented with fetal bovine serum (5 to 10%) and antibiotics. HCoVs and recombinant vaccinia viruses were propagated, titrated, and purified as described previously (58).

Cloning of plasmid DNAs and recombinant vaccinia viruses. To generate recombinant vaccinia viruses, the following plasmid DNAs were constructed using standard procedures. The details of construction and plasmid maps and sequences are available from the authors upon request.

To construct the recombinant vaccinia virus vHCoV-$PL1^{pro}$(−), two DNA fragments, designated EB-$PL1^{pro}$(−) and BF, were produced. These fragments together include HCoV-229E nucleotides (nt) 1 to 7006. The first fragment, EB-$PL1^{pro}$(−), includes HCoV-229E nt 1 to 5207, contains the $PL1^{pro}$ active-site Cys1054Ala mutation, and was constructed as follows. Plasmid DNA pEB (carrying HCoV-229E nucleotides 1 to 5207 preceded by one additional G nucleotide and the T7 RNA polymerase promoter) (59) was modified to introduce the $PL1^{pro}$ active-site Cys1054Ala mutation. Briefly, two PCRs were done using the vHCoV-inf-1 DNA (58) as a template. PCR1-$PL1^{pro}$(−) was done using primers OLV1/53 (5′-^{1221}TTGAAGGTGTCTCTGTTTGGAGAGTGAT^{1248}-3′) and JZ212 (5′-TATA*GGTCTC*AGGCGTTGTTATCCAATTGTTTGAGTA TC^{3427}-3′ (the BsaI restriction site is in italics, and the antisense Ala1054 codon is underlined). PCR2-$PL1^{pro}$(−) was done using primers JZ213 (5′-TATA*GGT CTC*ACGCCTGGGTTAACTCAGTTATGTTACAA^{3478}-3′ (the BsaI restriction site is in italics, and the Ala1054 codon is underlined) and Oli148 (5′-^{4218} GCAAGGTTCTCATTAGC^{4202}-3′). Both PCR products were cleaved with BsaI and ligated using T4 DNA ligase. The resulting ligation product was cleaved with SapI and Bsu36I and used to replace the corresponding SapI-Bsu36I fragment of plasmid DNA pEB. The resulting plasmid DNA, designated pEB-$PL1^{pro}$(−), was verified by sequence analysis. Plasmid DNA pEB-$PL1^{pro}$(−) was then cleaved with EagI and BglII and treated with alkaline phosphatase, and the DNA fragment EB-$PL1^{pro}$(−), containing HCoV-229E nt 1 to 5207 with the Cys1054Ala change, was gel purified. The second DNA fragment, BF, encompasses HCoV-229E nt 5176 to 7006 (59) and was generated using primers Bgl-up (5′-^{5176}AGTTGGTGTTATTGCTGATAAGGAC^{5200}-3′) and Fse-down (5′-^{7006} GACATAGGCCGGCCCTGTTGGTTGCACATTTGTTTTGGT^{6968}-3′). The PCR product PCR-BF was cleaved with BglII, and the resulting DNA fragment, BF, was ligated to the DNA fragment EB-$PL1^{pro}$(−). The ligation product [EB-$PL1^{pro}$(−)-BF] was cleaved with FseI, purified, and subsequently used in an in vitro ligation reaction with NotI-cleaved vaccinia virus vNotI/tk genomic DNA (41) and FseI-cleaved vaccinia virus vHCoV-inf-1 DNA. To rescue recombinant vaccinia virus vHCoV-$PL1^{pro}$(−), the ligation reaction was transfected without further purification into fowlpox-infected CV-1 cells as described previously (58). To identify a correct vHCoV-$PL1^{pro}$(−) clone, the recombinant vaccinia virus clones obtained were analyzed by Southern blotting, PCR, and sequence analysis of HCoV-229E nt 1 to 7100.

The recombinant vaccinia virus vHCoV-$PL2^{pro}$(−) was constructed similarly to the recombinant vaccinia virus vHCoV-$PL1^{pro}$(−) by in vitro ligation. First, plasmid DNA pEB (see above) was cleaved with EagI and BglII and treated with alkaline phosphatase, and the resulting DNA fragment, EB (HCoV-229E nt 1 to 5207), was gel purified. The DNA fragment PCR-BF encompassing HCoV-229E nt 5176 to 7006 (59) was modified to introduce the $PL2^{pro}$ active-site Cys1701Ala mutation as follows. PCR1-$PL2^{pro}$(−) was done with primers Bgl-up and JZ214 (5′-TATA*GGTCTC*AATGCATTATTATCACTAGTTTTTAACAC-3′ (the BsaI restriction site is in italics, and the antisense Ala1701 codon is underlined). PCR2-$PL2^{pro}$(−) was done using primer JZ215 (5′-TATA*GGTCTC*AG CATGGGTGAATGCTGTTTGTATTGCAC^{5420}-3′ (the BsaI restriction site is in italics, and the Ala1701 codon is underlined) and primer Fse-down. Both PCR products were cleaved with BsaI and ligated. The resulting ligation product, BF-$PL2^{pro}$(−), was cleaved with BglII and ligated to DNA fragment EB. The resulting ligation product [EB–BF-$PL2^{pro}$(−)] was cleaved with FseI, purified, and used in an in vitro ligation reaction with NotI-cleaved vaccinia virus vNotI/tk genomic DNA and FseI-cleaved vaccinia virus vHCoV-inf-1 DNA. To rescue recombinant vaccinia virus vHCoV-$PL2^{pro}$(−), the ligation reaction was transfected without further purification into fowlpox-infected CV-1 cells. To identify a correct vHCoV-$PL2^{pro}$(−) clone, the recombinant vaccinia virus clones obtained were analyzed by Southern blotting, PCR, and sequence analysis of HCoV-229E nt 1 to 7100.

To construct the recombinant vaccinia viruses vPL1(+)/PL2(+), vPL1(−)/PL2(+), and vPL1(+)/PL2(−), we first generated two plasmid DNAs, designated p7E1N and pFse3C. Plasmid DNA p7E1N was based on pBluescipt-KS(+) (Stratagene) and contained the bacteriophage T7 RNA polymerase promoter, the encephalomyocarditis virus internal ribosomal entry site (EMCV-IRES), and HCoV-229E nt 293 to 1485. Plasmid DNA pFse-3C contained HCoV-229E nt 6993 to 9187, a TAA stop codon, the HCoV-229E 3′ end (nt 27221 to 27277), a synthetic poly(A) sequence of 37 nt, and an EagI restriction site. The vaccinia virus inserts were assembled by in vitro ligation using three DNA fragments. Fragment 1 contained the T7 RNA polymerase promoter, the EMCV-IRES element, and HCoV-229E nt 293 to 1260 and was prepared from plasmid DNA p7E1N by EagI and SapI cleavage, alkaline phosphatase treatment, and gel purification. Three versions of fragment 2, encompassing HCoV-229E nt 1261 to 6995, were prepared by PCR using vaccinia virus genomic DNAs from vHCoV-inf-1, vHCoV-$PL1^{pro}$(−), and vHCoV-$PL2^{pro}$(−), respectively, as templates and subsequently cleaved with SapI and FseI. Depending on the DNA template used for PCR, the different versions of fragment 2 encoded either (i) two active PL^{pro}s, (ii) an inactive $PL1^{pro}$ and an active $PL2^{pro}$, or (iii) an active $PL1^{pro}$ and an inactive $PL2^{pro}$. Fragment 3 was prepared from plasmid DNA pFse3C by FseI and EagI cleavage, alkaline phosphatase treatment, and gel purification and encompassed HCoV-229E nt 6996 to 9187, a TAA stop codon, HCoV-229E nt 27221 to 27277, and a synthetic poly(A) sequence of 37 nt. After in vitro ligation of fragments 1, 2, and 3, the ligation products were ligated to NotI-cleaved vaccinia virus vNotI/tk genomic DNA. Rescue of recombinant vaccinia viruses vPL1(+)/PL2(+), vPL1(−)/PL2(+), and vPL1(+)/PL2(−) was done by transfection of the ligation products into fowlpox-infected CV-1 cells. The identities of recombinant vaccinia virus clones were confirmed by Southern blotting and sequence analysis.

Construction of recombinant vaccinia virus vHCoV-TaV-$PL1^{pro}$(−) was done by vaccinia virus-mediated homologous recombination using the *Escherichia coli* guanine phosphoribosyltransferase (*gpt*) gene as a marker for positive and negative selection, as described previously (30). We used plasmid DNA pRec-2 (30) for recombination with vHCoV-$PL1^{pro}$(−), resulting in the *gpt*-positive clone vHCoV-$PL1^{pro}$(−)-Rec-2. The second recombination was done with vHCoV-$PL1^{pro}$(−)-Rec-2 and plasmid DNA pEx2-TaV, which contains a 500-nt HindIII-

NotI fragment derived from vaccinia virus vNotI/tk, the T7 RNA polymerase promoter, one G nucleotide, HCoV-229E nt 1 to 616, the sequence encoding the *Thosea asigna virus* 2A-like autoprocessing peptide (16), and HCoV-229E nt 626 to 3323. The identity of the resulting recombinant vaccinia virus clone, vHCoV-TaV-PL1^{pro}(−), was verified by Southern blotting and sequence analysis of the region where recombination had occurred.

Rescue of recombinant HCoV-229E and HCoV-229E mutants. In vitro transcription from recombinant vaccinia virus genomic DNA using bacteriophage T7 RNA polymerase in the presence of an m7G(5′)ppp(5′)G cap analog was done as described previously (58, 59). To rescue recombinant HCoV-229E, BHK-HCoV-N cells were electroporated with full-length recombinant HCoV-229E RNA. On day 3, tissue culture supernatant was transferred to MRC-5 cells (passage 1).

RNA preparation, Northern blotting, RT-PCR, and sequence analysis. Poly(A)-containing RNA was isolated from BHK-HCoV-N cells that had been electroporated with recombinant HCoV-229E RNA or from infected MRC-5 cells using oligo(dT)$_{25}$ Dynabeads (Dynal, Oslo, Norway) as described previously (61). Northern blot analysis was done with a ^{32}P-labeled probe specific for the HCoV-229E nt 26297 to 27273, as described previously (60). Reverse transcription (RT)-PCR was done with Superscript II reverse transcriptase (Invitrogen). Sequence analysis of plasmid DNA, RT-PCR products, and recombinant vaccinia virus cDNA inserts was done by standard cycle-sequencing methods with an ABI 310 Prism Genetic Analyzer. Computer-assisted analysis of sequence data was facilitated by the Lasergene biocomputing software (DNASTAR).

Metabolic labeling, cell lysis, and immunoprecipitation. Vero cells (2×10^6) were coinfected with modified vaccinia virus Ankara (MVA) expressing T7 RNA polymerase (55) (multiplicity of infection [MOI] = 5) and one of the recombinant vaccinia viruses vNotI/tk, vPL1(+)/PL2(+), vPL1(−)/PL2(+), and vPL1(+)/PL2(−), respectively (MOI = 15). At 4.5 h postinfection (p.i.), the cells were labeled metabolically for 6 h using 100 μCi/ml of L-[^{35}S] in vitro cell-labeling mix (GE Healthcare) as described previously (65). At 10.5 h p.i., the radiolabeled cells were washed twice in ice-cold phosphate-buffered saline and lysed in 1 ml RIPA buffer (10 mM Tris-HCl, pH 7.4, 150 mM NaCl, 1% sodium deoxycholate, 1% Triton X-100, 0.1% sodium dodecyl sulfate [SDS]) containing protease inhibitors. After 30 min at 4°C, the lysates were centrifuged (10 min; 14,000 × *g*; 4°C) and the soluble protein fraction was mixed with 50 ml Pansorbin (Calbiochem) and incubated overnight at 4°C. The *Staphylococcus aureus* cells were pelleted, and the preabsorbed cell lysate was divided into two aliquots. Ten microliters of either an nsp1-specific antiserum, α-nsp1, or the corresponding preimmune serum was added to these aliquots, and the reaction mixtures were incubated for 2 h at 4°C. Next, 40 μl protein A-Sepharose bead suspension was added, and the reaction mixtures were incubated for 60 min at 4°C. Thereafter, the beads were pelleted, washed three times with 900 μl RIPA buffer, and resuspended in 40 μl Laemmli sample buffer, and the samples were heated for 5 min at 96°C. After a brief centrifugation step, the supernatant fractions were separated in SDS-17% polyacrylamide gels, and the precipitated proteins were visualized by autoradiography of the dried gels. The nsp1-specific serum used in these experiments was obtained by immunizing New Zealand White rabbits with a histidine-tagged form of nsp1 (HCoV-229E pp1a/pp1ab residues 1 to 111), which was expressed in *Escherichia coli* and purified under denaturing conditions.

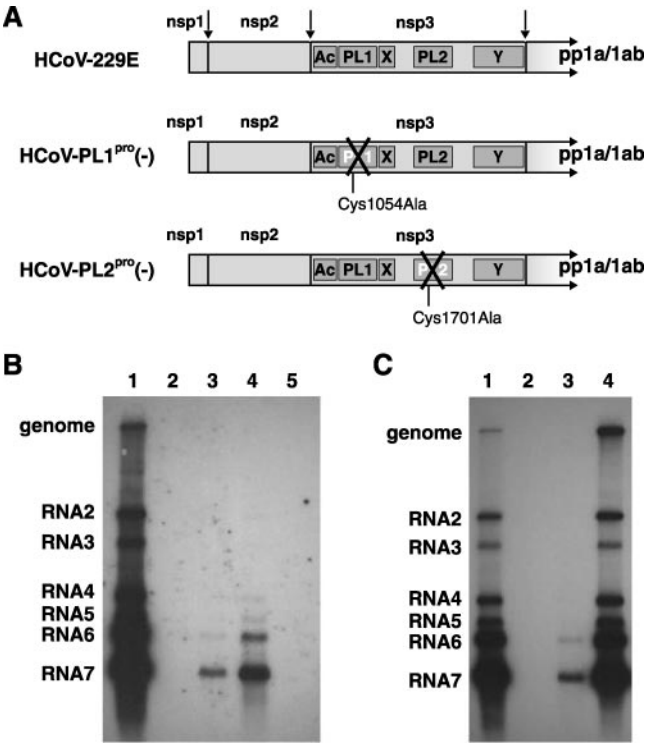

FIG. 2. Rescue of recombinant HCoV-229E with PL1^{pro} and PL2^{pro} active-site mutations. (A) The amino-terminal regions of HCoV-229E and the recombinant viruses HCoV-PL1^{pro}(−) and HCoV-PL2^{pro}(−) are shown schematically. Active-site amino acid substitutions engineered into the PL1^{pro} and PL2^{pro} domains are indicated. (B) Northern blot analysis of viral RNAs in MRC-5 cells infected with HCoV-229E (lane 1) or BHK-HCoV-N cells transfected with in vitro-transcribed HCoV-inf-1 RNA (lane 3), HCoV-PL1^{pro}(−) RNA (lane 4), and HCoV-PL2^{pro}(−) RNA (lane 5), respectively. Lane 2, mock-transfected BHK-HCoV-N cells. (C) Northern blot analysis of viral RNAs in MRC-5 cells infected with HCoV-229E (lane 1) or HCoV-PL1^{pro}(−) derived from passage 0 (lane 3) or passage 1 (lane 4) tissue culture supernatant. Lane 2, mock-infected MRC-5 cells. Ac, acidic domain; PL1, papain-like protease 1; X, ADP-ribose-1″-phosphatase; PL2, papain-like protease 2; Y, domain with conserved Cys/His residues and putative transmembrane regions.

RESULTS

PL1^{pro}, but not PL2^{pro}, activity is dispensable for HCoV-229E replication. We first determined if both PL^{pro} activities were required for HCoV-229E replication. To do this, two mutant HCoV-229E full-length cDNAs, in which one of the active-site cysteine codons was replaced by an alanine codon, were constructed (Fig. 2A). One mutant cDNA, vHCoV-PL1^{pro}(−), was designed to inactive the PL1^{pro} activity (Cys1054Ala), and the other, vHCoV-PL2^{pro}(−), was designed to inactivate the PL2^{pro} activity (Cys1701Ala). Both cDNA constructs were generated using our HCoV-229E full-length cDNA cloned in vaccinia virus (vHCoV-inf-1) as described in Materials and Methods. Full-length (wild-type and mutant) HCoV-229E RNAs were transcribed in vitro using genomic DNAs prepared from the recombinant vaccinia viruses vHCoV-inf-1, vHCoV-PL1^{pro}(−), and vHCoV-PL2^{pro}(−), respectively, as templates. Two days posttransfection of the in vitro-transcribed RNAs into BHK-HCoV-N cells, poly(A)-containing RNA was isolated and analyzed by Northern hybridization. As shown in Fig. 2B, viral RNAs were detectable in cells that had been transfected with HCoV-inf-1 (lane 3) and HCoV-PL1^{pro}(−) (lane 4) RNAs, but not in cells that had been transfected with HCoV-PL2^{pro}(−) RNA (lane 5). To rescue the recombinant viruses, tissue culture supernatants obtained from transfected BHK-HCoV-N cells were transferred to human embryonic lung fibroblasts (MRC-5 cells). As expected, after 3 days, a cytopathic effect was observed in monolayers of MRC-5 cells that had been inoculated with the supernatant from HCoV-inf-1 RNA-transfected BHK-HCoV-N cells, indicating successful rescue of HCoV-inf-1. Similarly, recombinant HCoV-PL1^{pro}(−) virus could be rescued, although the full cytopathic effect became apparent only after 5 days. The supernatants of the MRC-5 cells were also collected and passaged another four times on MRC-5 cells. Northern blot analysis of HCoV-PL1^{pro}(−)-infected MRC-5

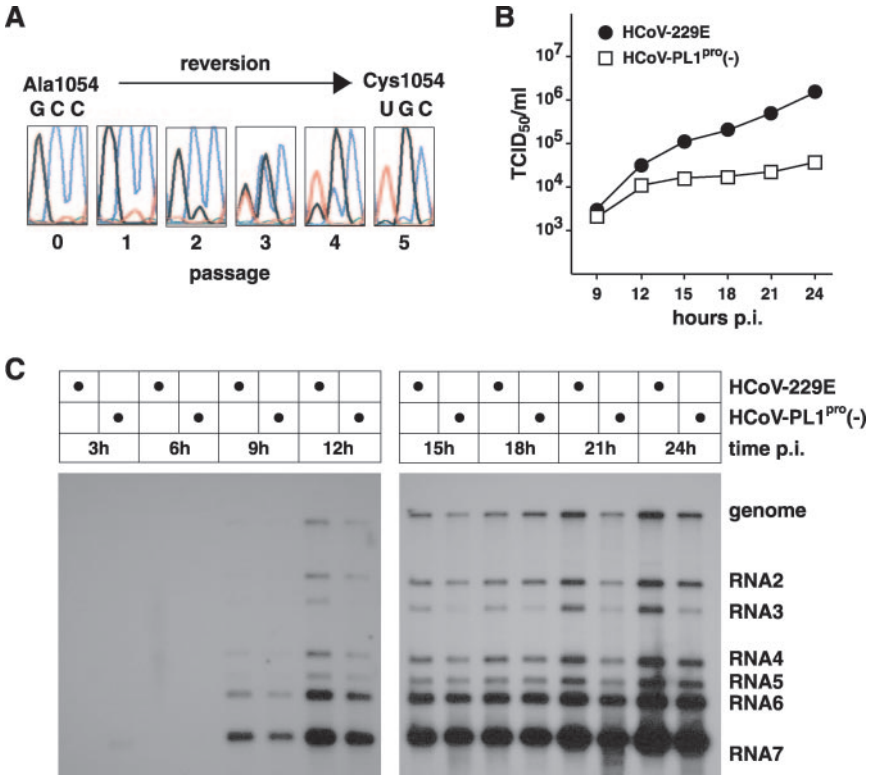

FIG. 3. Analysis of recombinant HCoV-PL1^{pro}(−). (A) Sequence analysis of recombinant HCoV-PL1^{pro}(−). After RT-PCR amplification using poly(A)-containing RNA isolated 3 days posttransfection or 2 days postinfection, the relevant genome region was sequenced. Passage 0 refers to BHK-HCoV-N cells transfected with HCoV-PL1^{pro}(−) RNA, and passages 1 to 5 refer to five consecutive passages of the HCoV-PL1^{pro}(−) mutant in MRC-5 cells. Shown are the sequence data for the active-site cysteine Cys1054Ala substitution. (B and C) Analysis of HCoV-PL1^{pro}(−) growth kinetics and RNA synthesis. MRC-5 cells (1×10^5) were infected (MOI = 1) with HCoV-229E or HCoV-PL1^{pro}(−) (passage 1 virus). At the indicated time points, viral titers were determined from the supernatants (B) and the accumulation of viral RNA was analyzed by Northern blotting (C). $TCID_{50}$, 50% tissue culture infective dose.

cells from passages 1 and 2 showed that all species of viral RNAs were produced (Fig. 2C, lanes 3 and 4). By contrast, in three independent experiments, we could neither detect HCoV-PL2^{pro}(−)-specific viral RNAs by Northern blot analysis nor rescue viable HCoV-PL2^{pro}(−) virus, indicating that inactivation of the PL2^{pro} activity is lethal.

Recombinant HCoV-PL1^{pro}(−) grows to reduced titers and reverts to the wild-type sequence. To verify that we had indeed rescued the original mutant, HCoV-PL1^{pro}(−), the relevant genome region was amplified by RT-PCR and sequenced. The data provided conclusive evidence for the presence of the introduced nucleotide changes UGC (Cys) to GCC (Ala) in viral RNA isolated from HCoV-PL1^{pro}(−) RNA-transfected BHK-HCoV-N cells (passage 0) and in viral RNAs isolated from infected MRC-5 cells at passages 1 and 2. However, at passage 3, a reversion of the GCC codon to the wild-type UGC codon became apparent, indicating that the introduced nucleotide changes were not stably maintained in tissue culture (Fig. 3A). Interestingly, the reversion pattern shown in Fig. 3A was highly reproducible, as the mixed sequence was detectable exactly at passage 3 in two separate experiments.

Although the reversion of HCoV-PL1^{pro}(−) to the wild-type sequence precluded the generation of a high-titer stock for detailed phenotypic analysis, we were able to collect passage 1-derived tissue culture supernatants from five individual rescue experiments, which allowed us to assess the growth kinetics of HCoV-PL1^{pro}(−). MRC-5 cells were infected with HCoV-229E or HCoV-PL1^{pro}(−) (MOI = 1), and viral RNAs and virus production were analyzed by Northern blotting and titration, respectively. Compared to HCoV-229E, HCoV-PL1^{pro}(−) displayed reduced growth kinetics and peak titers (Fig. 3B). Furthermore, the amounts of viral RNAs accumulating over time in HCoV-PL1^{pro}(−)-infected MRC-5 cells were reduced (Fig. 3C), indicating that the reduced viral titers most likely resulted from the reduced amounts or stability of viral RNAs.

Assessment of PL^{pro}-mediated nsp1-nsp2 cleavage. The reproducible reversion of HCoV-PL1^{pro}(−) to the wild-type sequence after three or four passages in tissue culture indicated to us that there was strong selection pressure for a proteolytically active PL1^{pro} enzyme. HCoV-229E PL1^{pro} can cleave pp1a/pp1ab at the nsp1-nsp2 and nsp2-nsp3 cleavage sites in vitro. Since PL2^{pro} dominates over PL1^{pro} at the latter site (67), we reasoned that an active PL1^{pro} enzyme might be primarily important for ensuring an efficient cleavage of the nsp1-nsp2 site. Indeed, nsp1-nsp2 cleavage site mutants of the group 1 CoVs transmissible gastroenteritis virus (20) and HCoV-229E (unpublished data), as well as the group 2a CoV MHV (14), were all revealed to display reduced growth kinetics similar to that of the HCoV-PL1^{pro}(−) mutant. Therefore,

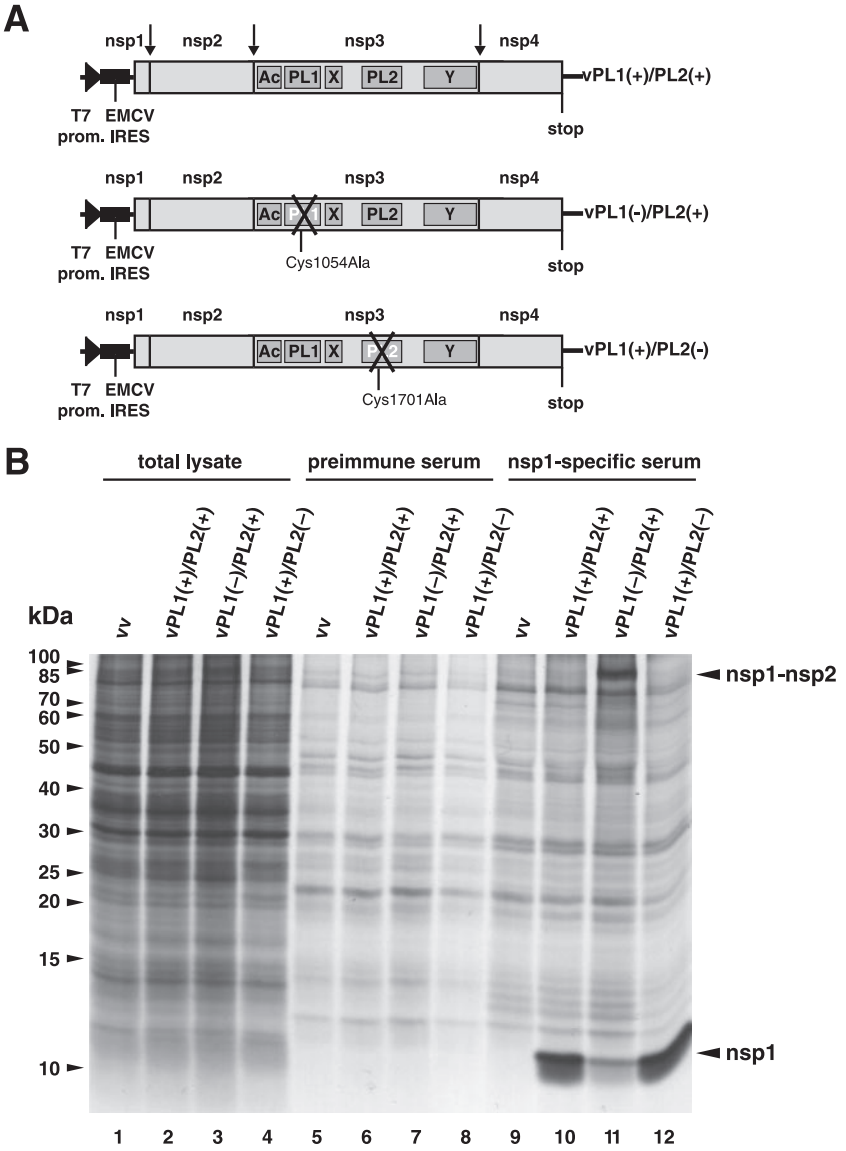

FIG. 4. Analysis of PL^{pro}-mediated nsp1-nsp2 cleavage. (A) Heterologous sequences engineered into the recombinant vaccinia viruses vPL1(+)/PL2(+), vPL1(−)/PL2(+), and vPL1(+)/PL2(−). The bacteriophage T7 RNA polymerase promoter (T7 prom.), the EMCV-IRES element, the HCoV-229E nsp1-to-nsp4 region, and the introduced active-site amino acid changes within the $PL1^{pro}$ and $PL2^{pro}$ domains are indicated. The vertical arrows depict PL^{pro} cleavage sites. (B) Vero cells (2×10^6) were coinfected with MVA expressing T7 RNA polymerase (MVA-T7) and vaccinia viruses vNotI/tk, vPL1(+)/PL2(+), vPL1(−)/PL2(+), and vPL1(+)/PL2(−), respectively. Infected cells were metabolically labeled from 4.5 to 10.5 h p.i., and pp1a/pp1ab processing products were immunoprecipitated using the nsp1-specific rabbit antiserum α-nsp1. The precipitated proteins were separated by SDS-polyacrylamide gel electrophoresis and visualized by autoradiography. The masses of marker proteins are indicated on the left. Lanes 1, 5, and 9, coinfection of MVA-T7 and vNotI/tk (vv); lanes 2, 6, and 10, coinfection of MVA-T7 and vPL1(+)/PL2(+); lanes 3, 7, and 11, coinfection of MVA-T7 and vPL1(−)/PL2(+); lanes 4, 8, and 12, coinfection of MVA-T7 and vPL1(+)/PL2(−). The radiolabeled proteins were analyzed either directly (lanes 1, 2, 3, and 4) or after immunoprecipitation with α-nsp1 serum (lanes 9, 10, 11, and 12) or the corresponding preimmune serum (lanes 5, 6, 7, and 8). Three microliters of each of the total lysates was loaded in lanes 1 to 4, whereas 500 μl of total cell lysate was used for the immunoprecipitation reactions analyzed in lanes 5 to 12. Ac, acidic domain; PL1, papain-like protease 1; X, ADP-ribose-1″-phosphatase; PL2, papain-like protease 2; Y, domain with conserved Cys/His residues and putative transmembrane regions.

it seemed reasonable to assess the cleavage efficiency of the nsp1-nsp2 site in the absence of an active $PL1^{pro}$ enzyme. Unfortunately, the relatively rapid reversion and the reduced growth kinetics of HCoV-$PL1^{pro}$(−) posed a significant obstacle to the analysis of the nsp1-nsp2 cleavage in HCoV-$PL1^{pro}$(−)-infected cells. To study the effects of $PL1^{pro}$ inactivation on the processing of the nsp1-nsp2 site, we therefore resorted to an alternative strategy. We cloned, in vaccina virus, the entire nsp1-to-nsp4 coding region (which includes all three PL^{pro} cleavage sites) downstream of a bacteriophage T7 RNA polymerase promoter and an EMCV-IRES element (Fig. 4A). To provide nsp4 with its authentic carboxy terminus, a translational stop codon was introduced directly downstream of the carboxy-terminal glutamine residue of nsp4. By in vitro liga-

tion, we cloned three recombinant vaccinia viruses in which either none or one of the PL^{pro} domains was inactivated: vPL1(+)/PL2(+) encoded active PL1^{pro} and PL2^{pro} enzymes, vPL1(−)/PL2(+) encoded an inactive PL1^{pro} (Cys1054Ala) and an active PL2^{pro}, and vPL1(+)/PL2(−) encoded an active PL1^{pro} and an inactive PL2^{pro} (Cys1701Ala). As shown in Fig. 4B, infection of Vero cells with these recombinant vaccinia viruses in combination with MVA expressing the bacteriophage T7 RNA polymerase enabled us to detect nsp1 expression by immunoprecipitation using an nsp1-specific rabbit antiserum. Consistent with the previously established role of PL1^{pro} in nsp1-nsp2 processing (28), fully processed nsp1 was readily detectable in vPL1(+)/PL2(+)- and vPL1(+)/PL2(−)-infected cells, indicating efficient processing of the nsp1-nsp2 cleavage site under these conditions (as observed in HCoV-229E-infected cells). Notably, fully processed nsp1 was also detectable in vPL1(−)/PL2(+)-infected cells, indicating that HCoV-229E PL2^{pro} can also mediate cleavage of the nsp1-nsp2 cleavage site. However, in this case, and in clear contrast to the other two constructs tested, the fraction of released nsp1 was strongly reduced and a protein corresponding to the size of unprocessed nsp1-nsp2 was precipitated. This led us to conclude that the PL2^{pro} activity can cleave both the nsp1-nsp2 and nsp2-nsp3 sites, although PL2^{pro}-mediated processing is less efficient than PL1^{pro}-mediated processing at the nsp1-nsp2 site.

Uncoupling of nsp1-nsp2 processing from viral PL^{pro} activities allows the recovery of PL1^{pro}-deficient HCoV-229E that can be stably propagated in cell culture. The results presented above were consistent with our hypothesis that the requirement for efficient processing of the nsp1-nsp2 site is a major driving force for the conservation of a proteolytically active PL1^{pro} in HCoV-229E. To further support this hypothesis, we decided to characterize a mutant in which the cleavage of the nsp1-nsp2 site was uncoupled from the activities of HCoV-229E-encoded PL^{pro}s. To this end, we replaced in the vHCoV-PL1^{pro}(−) cDNA the codons specifying the three consecutive glycine residues at the P3-to-P1 positions of the nsp1-nsp2 cleavage site with the coding sequence of a "2A-like" autoprocessing peptide derived from *Thosea asigna virus* (TaV-2A) (16) (see Materials and Methods). As a result of this replacement, PL^{pro}-mediated cleavage of the nsp1-nsp2 site was abolished, but the efficient release of nsp1 from pp1a/pp1ab was maintained by the activity of the TaV-2A element engineered at the interprotein junction. This element is proposed to mediate a translational termination and reinitiation at the carboxy-terminal glycine/proline residues of the TaV-2A peptide (Fig. 5A) (17), resulting in an nsp1 that is extended at its carboxy terminus by the short TaV-2A sequence (19 residues) and an nsp2 that is amino-terminally extended by an additional proline residue.

The genomic DNA of the vaccinia virus recombinant vHCoV-TaV-PL1^{pro}(−), encoding the TaV-2A element and an inactive PL1^{pro}, was used to produce full-length HCoV-TaV-PL1^{pro}(−) RNA. Recombinant HCoV-TaV-PL1^{pro}(−) could be rescued after RNA transfection into BHK-HCoV-N cells, and sequence analysis showed that both the TaV-2A element and the Cys1054Ala mutation were stably maintained in the HCoV-TaV-PL1^{pro}(−) genome (Fig. 5B). Even after 10 passages in tissue culture, the TaV-2A element and the Cys1054Ala mutation were maintained, and no extra mutations were detected by sequence analysis of approximately 1 kb around the TaV-2A element and the entire PL1^{pro} domain in the mutant progeny. The mutant virus displayed slightly delayed growth kinetics with titers that almost reached wild-type levels at 24 h postinfection (Fig. 5C) and were about 1 order of magnitude higher than those observed in HCoV-PL1^{pro}(−)-

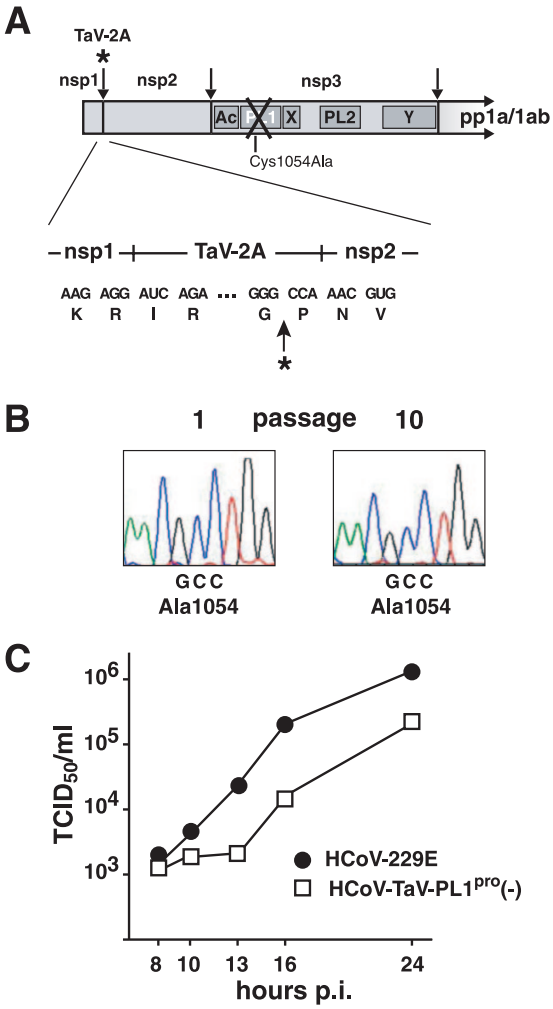

FIG. 5. Analysis of HCoV-TaV-PL1^{pro}(−). (A) The structure of the nsp1-to-nsp3 region of the recombinant HCoV-TaV-PL1^{pro}(−) is represented schematically. The positions of the TaV-2A sequence element inserted at the nsp1-nsp2 junction and the translational termination and reinitiation sites are shown. The arrow and asterisk indicate the TaV2a site in the upper part of the panel and the exact termination and reinitiation sites (termination at G, reinitiation at P) in the lower part of the panel. Note that the three carboxy-terminal Gly residues are deleted from the nsp1 sequence. (B) RT-PCR sequence analysis of HCoV-TaV-PL1^{pro}(−) derived from passages 1 and 10, respectively. The Cys1054Ala substitution is represented. (C) Growth kinetics of HCoV-TaV-PL1^{pro}(−). MRC-5 cells (1×10^5) were infected with HCoV-229E and HCoV-TaV-PL1^{pro}(−), respectively, at an MOI of 1. Virus titers are given as 50% tissue culture infective dosed ($TCID_{50}$) per ml of tissue culture supernatant at the indicated time points. The data points represent the means of two independent experiments. Ac, acidic domain; PL1, papain-like protease 1; X, ADP-ribose-1″-phosphatase; PL2, papain-like protease 2; Y, domain with conserved Cys/His residues and putative transmembrane regions.

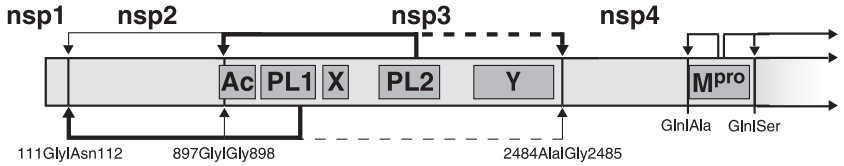

FIG. 6. PL^{pro}-mediated polyprotein processing in HCoV-229E. Shown are the PL^{pro}-mediated cleavages within the amino-terminal regions of the HCoV-229E polyproteins pp1a/pp1ab. Note that cleavages of the nsp1-nsp2 and nsp2-nsp3 sites can be mediated by either PL1^{pro} or PL2^{pro}, albeit with different efficiencies. The boldface lines indicate the dominant PL^{pro} activity at a given site, whereas thin lines indicate less efficient cleavages. The P1 and P1′ residues of the nsp1-nsp2 and nsp2-nsp3 cleavage sites have been determined experimentally under conditions where (i) nsp1-nsp2 cleavage was mediated by PL1^{pro} (28) and (ii) nsp2-nsp3 cleavage was mediated by either PL1^{pro} or PL2^{pro} (67). The predicted PL2^{pro} cleavage at the nsp3-nsp4 site is indicated by dotted lines. The predicted activity of PL2^{pro} and a potentially existing (but minor) activity of PL1^{pro} at the nsp3-nsp4 site remains to be studied. Ac, acidic domain; PL1, papain-like protease 1; X, ADP-ribose-1″-phosphatase; PL2, papain-like protease 2; Y, domain with conserved Cys/His residues and putative transmembrane regions.

infected cells. The data demonstrate that provision of efficient nsp1-nsp2 cleavage by an alternative mechanism lifts the selection pressure on the PL1^{pro}(−) mutant to revert to the wild-type sequence.

DISCUSSION

In this study, we used a reverse-genetics approach to dissect the involvement of PL^{pro} enzymes in the control of the polyprotein processing and replication of HCoV-229E, a prototypic group 1 CoV. There are a number of conclusions that can be drawn from our data. First, the proteolytic activity of PL1^{pro}, but not that of PL2^{pro}, appears to be dispensable for HCoV-229E replication. Second, there is, nevertheless, a strong selection pressure to maintain the proteolytic activity of PL1^{pro}, since recombinant HCoV-229E mutants lacking this activity reverted to the wild-type sequence within a few passages in tissue culture. Third, the proteolytic activity of PL1^{pro} is mainly required to efficiently process the nsp1-nsp2 cleavage site. Accordingly, if nsp1-nsp2 processing was functionally uncoupled from viral PL^{pro} activities, the PL1^{pro}(−) genotype could be stably maintained. Finally, we were able to demonstrate that PL2^{pro} is capable of processing the nsp1-nsp2 site, although this reaction proceeded less efficiently than that catalyzed by PL1^{pro}.

Our view of the PL^{pro}-mediated pp1a/pp1ab processing pathways in HCoV-229E as derived from previously published work (28, 29, 60, 67) and this study is summarized in Fig. 6. Among the CoVs characterized to date (7, 8, 14, 15, 27–29, 34, 36, 37, 60, 67) (Fig. 1), HCoV-229E seems to be unique in that the proteolytic release of nsp2 appears to be mediated at both its amino-terminal and carboxy-terminal processing sites by either of the two paralogous PL^{pro} domains (the dispensable PL1^{pro} or the essential PL2^{pro}). Remarkably, a functional dominance of one protease over the other was evident in both these reactions, with PL1^{pro} being dominant at the nsp1-nsp2 site and PL2^{pro} being dominant at the nsp2-nsp3 site. We originally discovered this phenomenon in a study in which we investigated the processing of the HCoV-229E nsp2-nsp3 site by expressing truncated proteins from the HCoV-229E nsp2-nsp3 region in reticulocyte lysates (67). The present study confirms the previous results and extends the data to include another cleavage site in a system that allows expression of the entire nsp1-to-nsp4 region in mammalian cells. Our data strongly suggest that the observed PL1^{pro}/PL2^{pro} redundancy at these two sites is functionally relevant for HCoV-229E replication, although it still remains technically challenging to extend these observations to the characterization of nsp1-nsp2 and nsp2-nsp3 processing in virus-infected cells. It remains to be seen whether the same redundancy applies to the processing of the nsp3-nsp4 site. The high conservation between all three cleavage sites in the HCoV-229E nsp1-to-nsp4 region (60, 67) and the predicted similarity of the substrate pockets of HCoV-229E PL1^{pro} and PL2^{pro} (54) seem to support this suggestion. If this were the case, then the essential PL2^{pro} could be expected to (heavily) dominate the dispensable PL1^{pro} in nsp3-nsp4 cleavage. As soon as suitable antibodies become available, the vaccinia virus-based HCoV-229E nsp1-to-nsp4 expression system established in this study may be used to investigate the precise mechanisms involved in the processing of the nsp3-nsp4 site.

The processing of the nsp1-to-nsp4 region appears to differ substantially between HCoV-229E and the group 2a CoV MHV, another virus with two PL^{pro}s. A recent study of MHV PL^{pro} processing (24) conclusively showed that, in infected cells, PL1^{pro} inactivation in the MHV genome results in unprocessed nsp1-nsp2 and nsp2-nsp3 sites, which have been shown by in vitro studies to be cleaved by PL1^{pro}. The observed processing defect in the mutant could not be compensated for by PL2^{pro}, possibly because, in this system, the latter enzyme is highly specialized for nsp3-nsp4 cleavage (35). Furthermore, PL1^{pro} inactivation caused a severe defect in MHV RNA synthesis, and the virus reverted rapidly to the wild-type sequence if the codon specifying the active site was replaced by Ala (24). In contrast, the equivalent HCoV-229E mutant was significantly less debilitated, and reversion occurred only after several passages in culture. Several other CoVs, e.g., SARS-CoV and IBV, employ only a single PL^{pro} to process the amino-proximal pp1a/pp1ab region. The regulation of the proteolytic-processing pathways in these two viruses has yet to be characterized at the same level as described above for MHV and HCoV-229E.

Comparative sequence analysis of CoVs with either one or two active PL^{pro}s suggest that the respective nsp1 and nsp2 proteins, although being released from equivalent positions in pp1a/pp1ab, may belong to different protein families (53) (A. E. Gorbalenya, unpublished observations). Also, the proteolytic release of homologous proteins may be controlled by different types of PL^{pro} activities in related CoVs, as exemplified by the proteolytic release of nsp1 in MHV versus SARS-CoV (4, 27). In total, four different functional patterns involv-

ing PL^{pro}s and nsp1 have been identified in CoVs: (i) no nsp1 and a single active PL2^{pro} (IBV), (ii) a group 2-specific nsp1 released by PL1^{pro} but not PL2^{pro} (MHV), (iii) a group 2-specific nsp1 released by PL2^{pro} (SARS-CoV), and (iv) a group 1-specific nsp1 released by PL1^{pro} and possibly assisted by PL2^{pro} (HCoV-229E). These four patterns represent the four major phylogenetic lineages of CoVs (23), indicating that they are separated by relatively large evolutionary distances and thus are likely to have emerged early in CoV evolution. Accordingly, when purified PL2^{pro} from the group 2b CoV SARS-CoV was tested on cognate and heterologous peptide substrates mimicking the respective nsp3-nsp4 cleavage sites, the processing efficiency correlated with the evolutionary distance between SARS-CoV and the respective virus from which a given substrate had been derived rather than the number of proteases encoded by the virus or any other parameter (26). Taken together, these studies suggest that the proteolytic-processing pathways of each of these CoV lineages need to be studied in more detail before a coherent model of the functional implications of differentially regulated expression strategies in this part of the CoV genome can be inferred.

Whereas PL2^{pro} is absolutely conserved among CoVs, PL1^{pro} is not. This observation has led to the hypothesis that CoVs initially evolved PL2^{pro} and later acquired PL1^{pro} through gene duplication (67). Since CoVs encoding one or two active PL^{pro}s phylogenetically intertwine, the repeated gain or loss, respectively, of PL1^{pro} during CoV evolution is a quite likely scenario. For example, it is possible that PL1^{pro} originated in the ancestor of the genus *Coronavirus* but was subsequently lost in a few branches, e.g., in groups 2b and 3. Alternatively, PL1^{pro} might have been introduced through independent duplications in the various branches at a later stage (67). Irrespective of which one of these scenarios is correct, each gain/loss of PL1^{pro} must have been driven by a change in the selection pressure imposed by the host(s). By unraveling a link between the efficiency of nsp1-nsp2 cleavage and the need for PL1^{pro} activity in HCoV-229E replication, we gained, for the first time, insight into possible selection forces that might have driven the evolution of CoV PL^{pro} activities. Our data led us to speculate that CoVs evolved a second (PL1^{pro}) activity in order to diversify and thereby elaborate the proteolytic control of gene expression of the amino-proximal pp1a/pp1ab region. In group 2a CoVs (prototype, MHV), the PL1^{pro} and PL2^{pro} domains and PL^{pro} cleavage sites diverged to an extent that allowed PL1^{pro} to take exclusive control of nsp1 and nsp2 production (24). By contrast, in HCoV-229E and probably other group 1 CoVs, similar or even overlapping substrate specificities have been retained, providing these viruses with some sort of "backup" mechanism to ensure the efficient release of their amino-terminal pp1a/pp1ab proteins. Besides the use of two protease activities with overlapping specificities, other factors may be employed to ensure differential processing kinetics of specific sites in HCoV-229E. Thus, for example, both the cleavage site sequences themselves and the spatial positions of these sites in the polyprotein in relation to the enzymes' active sites are likely to be involved in the control of the efficiency of substrate binding and cleavage. Most probably, such factors are also responsible for the observed kinetic differences in PL^{pro}-mediated polyprotein processing in SARS-CoV (27).

The observed reduction in the growth kinetics of HCoV-PL1^{pro}(−) and HCoV-TaV-PL1^{pro}(−) may indicate impaired functions of nsp1 to nsp4 (or their processing intermediates), resulting, for example, from an altered processing kinetics of the nsp1-nsp2 site. Similar defects have been reported for nsp1-nsp2 cleavage site mutants of MHV (14) and transmissible gastroenteritis virus (20). Alternatively, the extension of nsp1 and nsp2 with short TaV-2A sequences may have compromised the structures and/or functions of the respective proteins, thereby causing the observed defects in HCoV-229E replication. Although nsp1 to nsp4 colocalize with the replicase complex at perinuclear membranes within the host cell cytoplasm, a possible involvement in viral RNA synthesis has been demonstrated only for the hydrophobic, membrane-bound nsp4 (48). It is noteworthy that a carboxy-terminal truncation of nsp1 in MHV (11) and a complete deletion of nsp2 in MHV and SARS-CoV (25) were reported to be tolerated, indicating that nsp2 and parts of nsp1 are not essential for viral RNA synthesis. Moreover, an ADRPase-deficient HCoV-229E mutant was shown to replicate to nearly wild-type titers in tissue culture (43). The available information on nsp1 to nsp3, including the recently described involvement of SARS-CoV nsp1 in host cell mRNA degradation (33), the reported SARS-CoV PL^{pro} deubiquitination activity (5, 38), and sequence data on different isolates of bovine CoV (13), supports the idea that specific nsp1-to-nsp3 domains may be involved in virus-host interactions.

In summary, the study extends our knowledge of the complex CoV polyprotein-processing pathways. It shows that the proteolytic processing of the amino-proximal HCoV-229E pp1a/pp1ab region is tightly regulated by an interplay between two paralogous proteolytic activities with overlapping specificities. The functional characterization of the processing products derived from this region will be essential for comprehending the biological relevance of this sophisticated regulation of protein expression and its profound variation among CoVs from the four major lineages.

ACKNOWLEDGMENTS

This study was supported by the Swiss National Science Foundation, the European Commission (SARS-DTV SP22-CT-2004-511064), and the German Research Council (DFG).

REFERENCES

1. **Almazan, F., C. Galan, and L. Enjuanes.** 2004. The nucleoprotein is required for efficient coronavirus genome replication. J. Virol. **78:**12683–12688.
2. **Anand, K., G. J. Palm, J. R. Mesters, S. G. Siddell, J. Ziebuhr, and R. Hilgenfeld.** 2002. Structure of coronavirus main proteinase reveals combination of a chymotrypsin fold with an extra alpha-helical domain. EMBO J. **21:**3213–3224.
3. **Anand, K., J. Ziebuhr, P. Wadhwani, J. R. Mesters, and R. Hilgenfeld.** 2003. Coronavirus main proteinase (3CLpro) structure: basis for design of anti-SARS drugs. Science **300:**1763–1767.
4. **Baker, S. C., C. K. Shieh, L. H. Soe, M. F. Chang, D. M. Vannier, and M. M. Lai.** 1989. Identification of a domain required for autoproteolytic cleavage of murine coronavirus gene A polyprotein. J. Virol. **63:**3693–3699.
5. **Barretto, N., D. Jukneliene, K. Ratia, Z. Chen, A. D. Mesecar, and S. C. Baker.** 2005. The papain-like protease of severe acute respiratory syndrome coronavirus has deubiquitinating activity. J. Virol. **79:**15189–15198.
6. **Bhardwaj, K., L. Guarino, and C. C. Kao.** 2004. The severe acute respiratory syndrome coronavirus Nsp15 protein is an endoribonuclease that prefers manganese as a cofactor. J. Virol. **78:**12218–12224.
7. **Bonilla, P. J., S. A. Hughes, J. D. Pinon, and S. R. Weiss.** 1995. Characterization of the leader papain-like proteinase of MHV-A59: identification of a new in vitro cleavage site. Virology **209:**489–497.
8. **Bonilla, P. J., S. A. Hughes, and S. R. Weiss.** 1997. Characterization of a

second cleavage site and demonstration of activity in *trans* by the papain-like proteinase of the murine coronavirus mouse hepatitis virus strain A59. J. Virol. **71:**900–909.
9. **Brierley, I.** 1995. Ribosomal frameshifting viral RNAs. J. Gen. Virol. **76:** 1885–1892.
10. **Brierley, I., M. E. Boursnell, M. M. Binns, B. Bilimoria, V. C. Blok, T. D. Brown, and S. C. Inglis.** 1987. An efficient ribosomal frame-shifting signal in the polymerase-encoding region of the coronavirus IBV. EMBO J. **6:**3779–3785.
11. **Brockway, S. M., and M. R. Denison.** 2005. Mutagenesis of the murine hepatitis virus nsp1-coding region identifies residues important for protein processing, viral RNA synthesis, and viral replication. Virology **340:**209–223.
12. **Cheng, A., W. Zhang, Y. Xie, W. Jiang, E. Arnold, S. G. Sarafianos, and J. Ding.** 2005. Expression, purification, and characterization of SARS coronavirus RNA polymerase. Virology **335:**165–176.
13. **Chouljenko, V. N., X. Q. Lin, J. Storz, K. G. Kousoulas, and A. E. Gorbalenya.** 2001. Comparison of genomic and predicted amino acid sequences of respiratory and enteric bovine coronaviruses isolated from the same animal with fatal shipping pneumonia. J. Gen. Virol. **82:**2927–2933.
14. **Denison, M. R., B. Yount, S. M. Brockway, R. L. Graham, A. C. Sims, X. Lu, and R. S. Baric.** 2004. Cleavage between replicase proteins p28 and p65 of mouse hepatitis virus is not required for virus replication. J. Virol. **78:**5957–5965.
15. **Dong, S., and S. C. Baker.** 1994. Determinants of the p28 cleavage site recognized by the first papain-like cysteine proteinase of murine coronavirus. Virology **204:**541–549.
16. **Donnelly, M. L., L. E. Hughes, G. Luke, H. Mendoza, E. ten Dam, D. Gani, and M. D. Ryan.** 2001. The 'cleavage' activities of foot-and-mouth disease virus 2A site-directed mutants and naturally occurring '2A-like' sequences. J. Gen. Virol. **82:**1027–1041.
17. **Donnelly, M. L., G. Luke, A. Mehrotra, X. Li, L. E. Hughes, D. Gani, and M. D. Ryan.** 2001. Analysis of the aphthovirus 2A/2B polyprotein 'cleavage' mechanism indicates not a proteolytic reaction, but a novel translational effect: a putative ribosomal 'skip'. J. Gen. Virol. **82:**1013–1025.
18. **Egloff, M. P., F. Ferron, V. Campanacci, S. Longhi, C. Rancurel, H. Dutartre, E. J. Snijder, A. E. Gorbalenya, C. Cambillau, and B. Canard.** 2004. The severe acute respiratory syndrome-coronavirus replicative protein nsp9 is a single-stranded RNA-binding subunit unique in the RNA virus world. Proc. Natl. Acad. Sci. USA **101:**3792–3796.
19. **Egloff, M. P., H. Malet, A. Putics, M. Heinonen, H. Dutartre, A. Frangeul, A. Gruez, V. Campanacci, C. Cambillau, J. Ziebuhr, T. Ahola, and B. Canard.** 2006. Structural and functional basis for ADP-ribose and poly(ADP-ribose) binding by viral macro domains. J. Virol. **80:**8493–8502.
20. **Galan, C., L. Enjuanes, and F. Almazan.** 2005. A point mutation within the replicase gene differentially affects coronavirus genome versus minigenome replication. J. Virol. **79:**15016–15026.
21. **Gorbalenya, A. E., E. V. Koonin, A. P. Donchenko, and V. M. Blinov.** 1989. Coronavirus genome: prediction of putative functional domains in the nonstructural polyprotein by comparative amino acid sequence analysis. Nucleic Acids Res. **17:**4847–4861.
22. **Gorbalenya, A. E., E. V. Koonin, and M. M. Lai.** 1991. Putative papain-related thiol proteases of positive-strand RNA viruses. Identification of rubi- and aphthovirus proteases and delineation of a novel conserved domain associated with proteases of rubi-, alpha- and coronaviruses. FEBS Lett. **288:**201–205.
23. **Gorbalenya, A. E., E. J. Snijder, and W. J. Spaan.** 2004. Severe acute respiratory syndrome coronavirus phylogeny: toward consensus. J. Virol. **78:**7863–7866.
24. **Graham, R. L., and M. R. Denison.** 2006. Replication of murine hepatitis virus is regulated by papain-like proteinase 1 processing of nonstructural proteins 1, 2, and 3. J. Virol. **80:**11610–11620.
25. **Graham, R. L., A. C. Sims, S. M. Brockway, R. S. Baric, and M. R. Denison.** 2005. The nsp2 replicase proteins of murine hepatitis virus and severe acute respiratory syndrome coronavirus are dispensable for viral replication. J. Virol. **79:**13399–13411.
26. **Han, Y. S., G. G. Chang, C. G. Juo, H. J. Lee, S. H. Yeh, J. T. Hsu, and X. Chen.** 2005. Papain-like protease 2 (PLP2) from severe acute respiratory syndrome coronavirus (SARS-CoV): expression, purification, characterization, and inhibition. Biochemistry **44:**10349–10359.
27. **Harcourt, B. H., D. Jukneliene, A. Kanjanahaluethai, J. Bechill, K. M. Severson, C. M. Smith, P. A. Rota, and S. C. Baker.** 2004. Identification of severe acute respiratory syndrome coronavirus replicase products and characterization of papain-like protease activity. J. Virol. **78:**13600–13612.
28. **Herold, J., A. E. Gorbalenya, V. Thiel, B. Schelle, and S. G. Siddell.** 1998. Proteolytic processing at the amino terminus of human coronavirus 229E gene 1-encoded polyproteins: identification of a papain-like proteinase and its substrate. J. Virol. **72:**910–918.
29. **Herold, J., S. G. Siddell, and A. E. Gorbalenya.** 1999. A human RNA viral cysteine proteinase that depends upon a unique Zn2+-binding finger connecting the two domains of a papain-like fold. J. Biol. Chem. **274:**14918–14925.
30. **Hertzig, T., E. Scandella, B. Schelle, J. Ziebuhr, S. G. Siddell, B. Ludewig, and V. Thiel.** 2004. Rapid identification of coronavirus replicase inhibitors using a selectable replicon RNA. J. Gen. Virol. **85:**1717–1725.
31. **Ivanov, K. A., T. Hertzig, M. Rozanov, S. Bayer, V. Thiel, A. E. Gorbalenya, and J. Ziebuhr.** 2004. Major genetic marker of nidoviruses encodes a replicative endoribonuclease. Proc. Natl. Acad. Sci. USA **101:**12694–12699.
32. **Joseph, J. S., K. S. Saikatendu, V. Subramanian, B. W. Neuman, A. Brooun, M. Griffith, K. Moy, M. K. Yadav, J. Velasquez, M. J. Buchmeier, R. C. Stevens, and P. Kuhn.** 2006. Crystal structure of nonstructural protein 10 from the severe acute respiratory syndrome coronavirus reveals a novel fold with two zinc-binding motifs. J. Virol. **80:**7894–7901.
33. **Kamitani, W., K. Narayanan, C. Huang, K. Lokugamage, T. Ikegami, N. Ito, H. Kubo, and S. Makino.** 2006. Severe acute respiratory syndrome coronavirus nsp1 protein suppresses host gene expression by promoting host mRNA degradation. Proc. Natl. Acad. Sci. USA **103:**12885–12890.
34. **Kanjanahaluethai, A., and S. C. Baker.** 2000. Identification of mouse hepatitis virus papain-like proteinase 2 activity. J. Virol. **74:**7911–7921.
35. **Kanjanahaluethai, A., D. Jukneliene, and S. C. Baker.** 2003. Identification of the murine coronavirus MP1 cleavage site recognized by papain-like proteinase 2. J. Virol. **77:**7376–7382.
36. **Lim, K. P., and D. X. Liu.** 1998. Characterization of the two overlapping papain-like proteinase domains encoded in gene 1 of the coronavirus infectious bronchitis virus and determination of the C-terminal cleavage site of an 87-kDa protein. Virology **245:**303–312.
37. **Lim, K. P., L. F. Ng, and D. X. Liu.** 2000. Identification of a novel cleavage activity of the first papain-like proteinase domain encoded by open reading frame 1a of the coronavirus avian infectious bronchitis virus and characterization of the cleavage products. J. Virol. **74:**1674–1685.
38. **Lindner, H. A., N. Fotouhi-Ardakani, V. Lytvyn, P. Lachance, T. Sulea, and R. Menard.** 2005. The papain-like protease from the severe acute respiratory syndrome coronavirus is a deubiquitinating enzyme. J. Virol. **79:**15199–15208.
39. **Marra, M. A., S. J. Jones, C. R. Astell, R. A. Holt, A. Brooks-Wilson, Y. S. Butterfield, J. Khattra, J. K. Asano, S. A. Barber, S. Y. Chan, A. Cloutier, S. M. Coughlin, D. Freeman, N. Girn, O. L. Griffith, S. R. Leach, M. Mayo, H. McDonald, S. B. Montgomery, P. K. Pandoh, A. S. Petrescu, A. G. Robertson, J. E. Schein, A. Siddiqui, D. E. Smailus, J. M. Stott, G. S. Yang, F. Plummer, A. Andonov, H. Artsob, N. Bastien, K. Bernard, T. F. Booth, D. Bowness, M. Czub, M. Drebot, L. Fernando, R. Flick, M. Garbutt, M. Gray, A. Grolla, S. Jones, H. Feldmann, A. Meyers, A. Kabani, Y. Li, S. Normand, U. Stroher, G. A. Tipples, S. Tyler, R. Vogrig, D. Ward, B. Watson, R. C. Brunham, M. Krajden, M. Petric, D. M. Skowronski, C. Upton, and R. L. Roper.** 2003. The genome sequence of the SARS-associated coronavirus. Science **300:**1399–1404.
40. **Matthes, N., J. R. Mesters, B. Coutard, B. Canard, E. J. Snijder, R. Moll, and R. Hilgenfeld.** 2006. The non-structural protein Nsp10 of mouse hepatitis virus binds zinc ions and nucleic acids. FEBS Lett. **580:**4143–4149.
41. **Merchlinsky, M., and B. Moss.** 1992. Introduction of foreign DNA into the vaccinia virus genome by in vitro ligation: recombination-independent selectable cloning vectors. Virology **190:**522–526.
42. **Minskaia, E., T. Hertzig, A. E. Gorbalenya, V. Campanacci, C. Cambillau, B. Canard, and J. Ziebuhr.** 2006. Discovery of an RNA virus 3′→5′ exoribonuclease that is critically involved in coronavirus RNA synthesis. Proc. Natl. Acad. Sci. USA **103:**5108–5113.
43. **Putics, A., W. Filipowicz, J. Hall, A. E. Gorbalenya, and J. Ziebuhr.** 2005. ADP-ribose-1″-monophosphatase: a conserved coronavirus enzyme that is dispensable for viral replication in tissue culture. J. Virol. **79:**12721–12731.
44. **Ratia, K., K. S. Saikatendu, B. D. Santarsiero, N. Barretto, S. C. Baker, R. C. Stevens, and A. D. Mesecar.** 2006. Severe acute respiratory syndrome coronavirus papain-like protease: structure of a viral deubiquitinating enzyme. Proc. Natl. Acad. Sci. USA **103:**5717–5722.
45. **Rota, P. A., M. S. Oberste, S. S. Monroe, W. A. Nix, R. Campagnoli, J. P. Icenogle, S. Penaranda, B. Bankamp, K. Maher, M. H. Chen, S. Tong, A. Tamin, L. Lowe, M. Frace, J. L. DeRisi, Q. Chen, D. Wang, D. D. Erdman, T. C. Peret, C. Burns, T. G. Ksiazek, P. E. Rollin, A. Sanchez, S. Liffick, B. Holloway, J. Limor, K. McCaustland, M. Olsen-Rasmussen, R. Fouchier, S. Gunther, A. D. Osterhaus, C. Drosten, M. A. Pallansch, L. J. Anderson, and W. J. Bellini.** 2003. Characterization of a novel coronavirus associated with severe acute respiratory syndrome. Science **300:**1394–1399.
46. **Saikatendu, K. S., J. S. Joseph, V. Subramanian, T. Clayton, M. Griffith, K. Moy, J. Velasquez, B. W. Neuman, M. J. Buchmeier, R. C. Stevens, and P. Kuhn.** 2005. Structural basis of severe acute respiratory syndrome coronavirus ADP-ribose-1′-phosphate dephosphorylation by a conserved domain of nsP3. Structure **13:**1665–1675.
47. **Sawicki, S. G., D. L. Sawicki, and S. G. Siddell.** 2006. A contemporary view of coronavirus transcription. J. Virol. **81:**20–29.
48. **Sawicki, S. G., D. L. Sawicki, D. Younker, Y. Meyer, V. Thiel, H. Stokes, and S. G. Siddell.** 2005. Functional and genetic analysis of coronavirus replicase-transcriptase proteins. PLoS Pathog. **1:**e39.
49. **Schelle, B., N. Karl, B. Ludewig, S. G. Siddell, and V. Thiel.** 2005. Selective replication of coronavirus genomes that express nucleocapsid protein. J. Virol. **79:**6620–6630.
50. **Seybert, A., A. Hegyi, S. G. Siddell, and J. Ziebuhr.** 2000. The human

coronavirus 229E superfamily 1 helicase has RNA and DNA duplex-unwinding activities with 5′-to-3′ polarity. RNA **6:**1056–1068.
51. **Shi, S. T., and M. M. Lai.** 2005. Viral and cellular proteins involved in coronavirus replication. Curr. Top. Microbiol. Immunol. **287:**95–131.
52. **Siddell, S. G., J. Ziebuhr, and E. J. Snijder.** 2005. Coronaviruses, toroviruses, and arteriviruses, p. 823–856. *In* B. W. J. Mahy and V. ter Meulen (ed.), Topley and Wilson's microbiology and microbial infections, 10th ed., vol. Virology 1. Hodder Arnold, London, United Kingdom.
53. **Snijder, E. J., P. J. Bredenbeek, J. C. Dobbe, V. Thiel, J. Ziebuhr, L. L. Poon, Y. Guan, M. Rozanov, W. J. Spaan, and A. E. Gorbalenya.** 2003. Unique and conserved features of genome and proteome of SARS-coronavirus, an early split-off from the coronavirus group 2 lineage. J. Mol. Biol. **331:**991–1004.
54. **Sulea, T., H. A. Lindner, E. O. Purisima, and R. Menard.** 2006. Binding site-based classification of coronaviral papain-like proteases. Proteins **62:** 760–775.
55. **Sutter, G., M. Ohlmann, and V. Erfle.** 1995. Non-replicating vaccinia vector efficiently expresses bacteriophage T7 RNA polymerase. FEBS Lett. **371:** 9–12.
56. **Sutton, G., E. Fry, L. Carter, S. Sainsbury, T. Walter, J. Nettleship, N. Berrow, R. Owens, R. Gilbert, A. Davidson, S. Siddell, L. L. Poon, J. Diprose, D. Alderton, M. Walsh, J. M. Grimes, and D. I. Stuart.** 2004. The nsp9 replicase protein of SARS-coronavirus, structure and functional insights. Structure **12:**341–353.
57. **Teng, H., J. D. Pinon, and S. R. Weiss.** 1999. Expression of murine coronavirus recombinant papain-like proteinase: efficient cleavage is dependent on the lengths of both the substrate and the proteinase polypeptides. J. Virol. **73:**2658–2666.
58. **Thiel, V., J. Herold, B. Schelle, and S. G. Siddell.** 2001. Infectious RNA transcribed in vitro from a cDNA copy of the human coronavirus genome cloned in vaccinia virus. J. Gen. Virol. **82:**1273–1281.
59. **Thiel, V., J. Herold, B. Schelle, and S. G. Siddell.** 2001. Viral replicase gene products suffice for coronavirus discontinuous transcription. J. Virol. **75:** 6676–6681.
60. **Thiel, V., K. A. Ivanov, A. Putics, T. Hertzig, B. Schelle, S. Bayer, B. Weissbrich, E. J. Snijder, H. Rabenau, H. W. Doerr, A. E. Gorbalenya, and J. Ziebuhr.** 2003. Mechanisms and enzymes involved in SARS coronavirus genome expression. J. Gen. Virol. **84:**2305–2315.
61. **Thiel, V., A. Rashtchian, J. Herold, D. M. Schuster, N. Guan, and S. G. Siddell.** 1997. Effective amplification of 20-kb DNA by reverse transcription PCR. Anal. Biochem. **252:**62–70.
62. **Thiel, V., and S. G. Siddell.** 2005. Reverse genetics of coronaviruses using vaccinia virus vectors. Curr. Top. Microbiol. Immunol. **287:**199–227.
63. **Zhai, Y., F. Sun, X. Li, H. Pang, X. Xu, M. Bartlam, and Z. Rao.** 2005. Insights into SARS-CoV transcription and replication from the structure of the nsp7-nsp8 hexadecamer. Nat. Struct. Mol. Biol. **12:**980–986.
64. **Ziebuhr, J.** 2005. The coronavirus replicase. Curr. Top. Microbiol. Immunol. **287:**57–94.
65. **Ziebuhr, J., J. Herold, and S. G. Siddell.** 1995. Characterization of a human coronavirus (strain 229E) 3C-like proteinase activity. J. Virol. **69:**4331–4338.
66. **Ziebuhr, J., E. J. Snijder, and A. E. Gorbalenya.** 2000. Virus-encoded proteinases and proteolytic processing in the Nidovirales. J. Gen. Virol. **81:**853–879.
67. **Ziebuhr, J., V. Thiel, and A. E. Gorbalenya.** 2001. The autocatalytic release of a putative RNA virus transcription factor from its polyprotein precursor involves two paralogous papain-like proteases that cleave the same peptide bond. J. Biol. Chem. **276:**33220–33232.